Excitonic effects in oxyhalide scintillating host compounds

G. Shwetha, V. Kanchana, and M. C. Valsakumar

Citation: Journal of Applied Physics **116**, 133510 (2014); doi: 10.1063/1.4896831
View online: http://dx.doi.org/10.1063/1.4896831
View Table of Contents: http://scitation.aip.org/content/aip/journal/jap/116/13?ver=pdfcov
Published by the AIP Publishing

Excitonic effects in oxyhalide scintillating host compounds

G. Shwetha,[1] V. Kanchana,[1,a)] and M. C. Valsakumar[2]
[1]*Department of Physics, Indian Institute of Technology Hyderabad, Ordnance Factory Estate, Yeddumailaram 502 205, Telangana, India*
[2]*School of Engineering Sciences and Technology (SEST), University of Hyderabad, Prof. C. R. Rao Road, Gachibowli, Hyderabad 500 046, Telangana, India*

(Received 27 August 2014; accepted 19 September 2014; published online 2 October 2014)

Ab-initio calculations based on density functional theory have been performed to study the electronic, optical, mechanical, and vibrational properties of scintillator host compounds YOX (X = F, Cl, Br, and I). Semiempirical dispersion correction schemes are used to find the effect of van der Waals forces on these layered compounds and we found this effect to be negligible except for YOBr. Calculations of phonons and elastic constants showed that all the compounds studied here are both dynamically and mechanically stable. YOF and YOI are found to be indirect band gap insulators while YOCl and YOBr are direct band gap insulators. The band gap is found to decrease as we move from fluorine to iodine, while the calculated refractive index shows the opposite trend. As the band gap decreases on going down the periodic table from YOF to YOI, the luminescence increases. The excitonic binding energy calculated, within the effective mass approximation, is found to be more for YOF than the remaining compounds, suggesting that the excitonic effect to be more in YOF than the other compounds. The optical properties are calculated within the Time-Dependent Density Functional Theory (TDDFT) and compared with results obtained within the random phase approximation. The TDDFT calculations, using the newly developed bootstrap exchange-correlation kernel, showed significant excitonic effects in all the compounds studied here. © *2014 AIP Publishing LLC*. [http://dx.doi.org/10.1063/1.4896831]

I. INTRODUCTION

Rare earth halides doped with cerium are reported to have high luminosity[1–4] with short decay time. However, these materials are difficult to be used because of their hygroscopic nature. It is possible to change the degree of hygroscopicity by doping oxyhalides with different rare earth elements–room temperature scintillation properties, x-ray excited emission spectra, and scintillation decay curves[5] of cerium doped oxyhalides show that doping reduces the hygroscopic character of the host; hygroscopic nature of these rare earth oxyhalide is inversely related to the size of the rare earth element. However, this doping not only changes the hygroscopic character but also the optical properties of the material. The reasons behind these changes are not yet fully explored.

Knowledge of electronic structure and dynamical properties of the host compounds is the key to understand these changes in the optoelectronic properties upon doping.[6] In order to understand the underlying mechanism responsible for change in the luminescence, we have investigated the electronic and optical properties of the host compounds YOX (X = F, Cl, Br, and I) particularly with the inclusion of excitonic effect which, as we shall show, plays a major role in these materials. The organization of the paper is as follows. After a brief description of the technical details of our calculations in Sec. II, the results are discussed in Sec. III. Apart from a discussion of the crystal structure and electronic structure, results of vibrational and elastic constant calculations are presented to show that all the materials considered here are both dynamically and mechanically stable. This is followed by a detailed account of the results on the study of optical properties using Random Phase Approximation (RPA) as well as Time Dependent Density functional Theory (TDDFT). Finally the conclusions of the study are presented in Sec. IV.

II. DETAILS OF CALCULATION

The compound YOF forms in a crystal structure with space group $R\bar{3}m$ (166) containing two formula units per unit cell in which the atoms are placed at sites with Wyckoff positions 2(c) in the rhombohedral representation and 6(c) in the hexagonal representation.[7,8] The other three compounds crystallize in the PbFCl type crystal structure with space group P4/nmm (129). Y and X(Cl, Br, and I) are placed at the 2(c) Wyckoff positions with site symmetry C_{4v}[9,10] and oxygen at 2(a) position with site symmetry D_{2d}. In YOX crystal structure, each rare earth ion is co-ordinated to 4 Oxygen and 4 Halide ions.

Ab-initio calculations are performed using pseudopotential CASTEP (Cambridge Series of Total Energy Package)[11–13] code and Full-potential linear augmented plane-wave method as implemented in the WIEN2k[14,15] and Elk code.[16] Geometry optimization was performed using CASTEP. In order to study the effect of different approximations to the exchange-correlation functional on the final geometry, calculations were performed with three different exchange-correlation functionals—Ceperley and Alder,[17]

a)Author to whom correspondence should be addressed. Electronic mail: kanchana@iith.ac.in

and Perdew and Zunger[18] parametrized local density approximation (LDA), and Perdew-Burke-Ernzerhof (PBE)[19] parametrized generalized gradient approximation (GGA). Since these compounds have a layered structure (shown in Fig. 1 with Y, O, and X (F, Cl, Br, and I) with atoms forming layers perpendicular to the *c*-axis, we have also used the semi-empirical dispersion corrected DFT (DFT-D)[20–26] to study the effect of van der Waals forces.

The electronic structure was studied using the Full-potential linearized augmented plane-wave method. For this, the experimental lattice parameter and the theoretically optimized lattice positions were used. A mesh of $12 \times 12 \times 6$ *k*-points in the irreducible Brillouin zone (IBZ) was used to achieve convergence. Along with the LDA and GGA exchange-correlation functionals, we have also performed calculations using the Tran and Blaha modified Becke-Johnson (TB-mBJ)[27,28] functional for calculating various properties of all the compounds. We have determined the vibrational frequencies and elastic constants to study the dynamical and mechanical stability of these compounds. Vibrational properties are calculated by using norm conserving pseudopotentials with an energy cutoff of 750 eV and a *k*-mesh of $8 \times 8 \times 4$ for YOBr, YOCl, YOI and 850 eV and $8 \times 8 \times 2$ for the YOF in the hexagonal representation. The elastic constants are calculated for the optimized crystal structure by using the volume-conserving strain technique[29] as implemented in CASTEP code. Optical properties are first investigated using RPA, and then with TDDFT in order to study the excitonic effects in the optical spectra. The TDDFT calculations were carried out with bootstrap kernel[30,31] as the bootstrap calculations are computationally less expensive and give results of comparable quality as the Bethe-Salpeter equation. As it is well known that DFT generally underestimates the band gap,[32] we have applied scissors correction based on the experimental gap to account for this shortcoming.

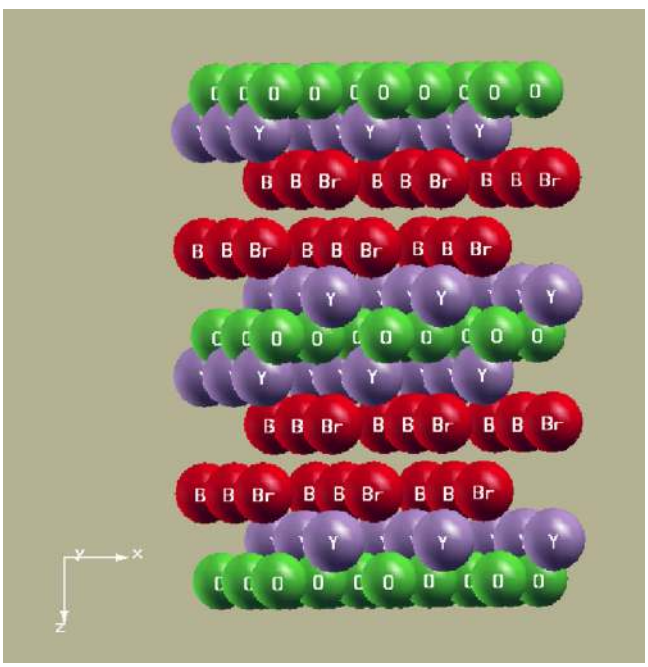

FIG. 1. Layered structure of YOBr compounds in tetragonal crystal structure. The layers are stacked along z-direction.

III. RESULTS AND DISCUSSIONS

A. Structure and electronic properties

The geometry optimization has been performed using both LDA and GGA. In order to find the effect of van der Waals forces in these layered compounds, dispersion corrected methods (OBS, TS, and Grimme) are also used. The volumes computed using the LDA and the GGA are comparable to the experiments, implying that the effect of van-der-Waals interactions is rather small in these compounds. An exception to this is YOBr, in which van der Waals corrections play an important role.

The calculated band gaps, obtained using various functionals, are given in Table I. As expected, the TB-mBJ functional gives values close to experiments. Interestingly, we observe that the band gap decreases on moving from fluorine to iodine in these compounds leading to an increase in the luminescence. The calculated band structures along the high symmetry directions (computed using the TB-mBJ functional) are shown in Fig. 2. YOF and YOI have an indirect band gap and YOCl, YOBr are direct band gap insulators. On comparing the band structures of these compounds, we find that hybridization between the bands is higher in the case of YOCl, YOBr, YOI, and not so much in YOF. This might be due to the fact that the difference in the value of electronegativity between fluorine and oxygen atoms is large in YOF. Another factor could also be that the radius of the F^- atom is smaller than other halides leading to reduced hopping, and hybridization between between F-*p* and O-*p* orbitals.

The partial density of states, calculated using the TB-mBJ functional, is shown in Fig. 3. In order to understand the predominant atomic and orbital character of the electronic states, we have divided the states into five blocks. The first block, i.e., the conduction band, is due to the hybridization of Y-*d*, O-*p*, and X-*d* states. The second block, i.e., the valence bands, is due the mixed states of O-*p* and X-*p* states in all the compounds. We observe the top most valence band of YOF to be nonoverlapping and are formed by the O-*p* and F-*p*. The third block is formed by O-*s* states mixed with Y-*p* states in the case of YOF and X-*s* states in case of the remaining compounds. The fourth block is of Y-*p* with small contribution from O-*s* and F-*s* states in case of YOF and O-*s* and Y-*p* mixed states in case of other compounds. The fifth block is due to the F-*s* states hybridized with Y-*p* states in case of YOF and Y-*p*, O-*s* states in the

TABLE I. Calculated band gap of YOX (X = F, Cl, Br, and I) compounds in eV using LDA, GGA and TB-mBJ functionals using WIEN2k.

	YOF	YOCl	YOBr	YOI
LDA	4.9	4.5	3.6	3.4
GGA	5.1	4.9	4.4	3.6
TB-mBJ	6.8	6.2	5.5	4.5
Others[6]	5.0	4.0	3.7	2.6
exp[33,34]	7.2, 5.6	…	…	…

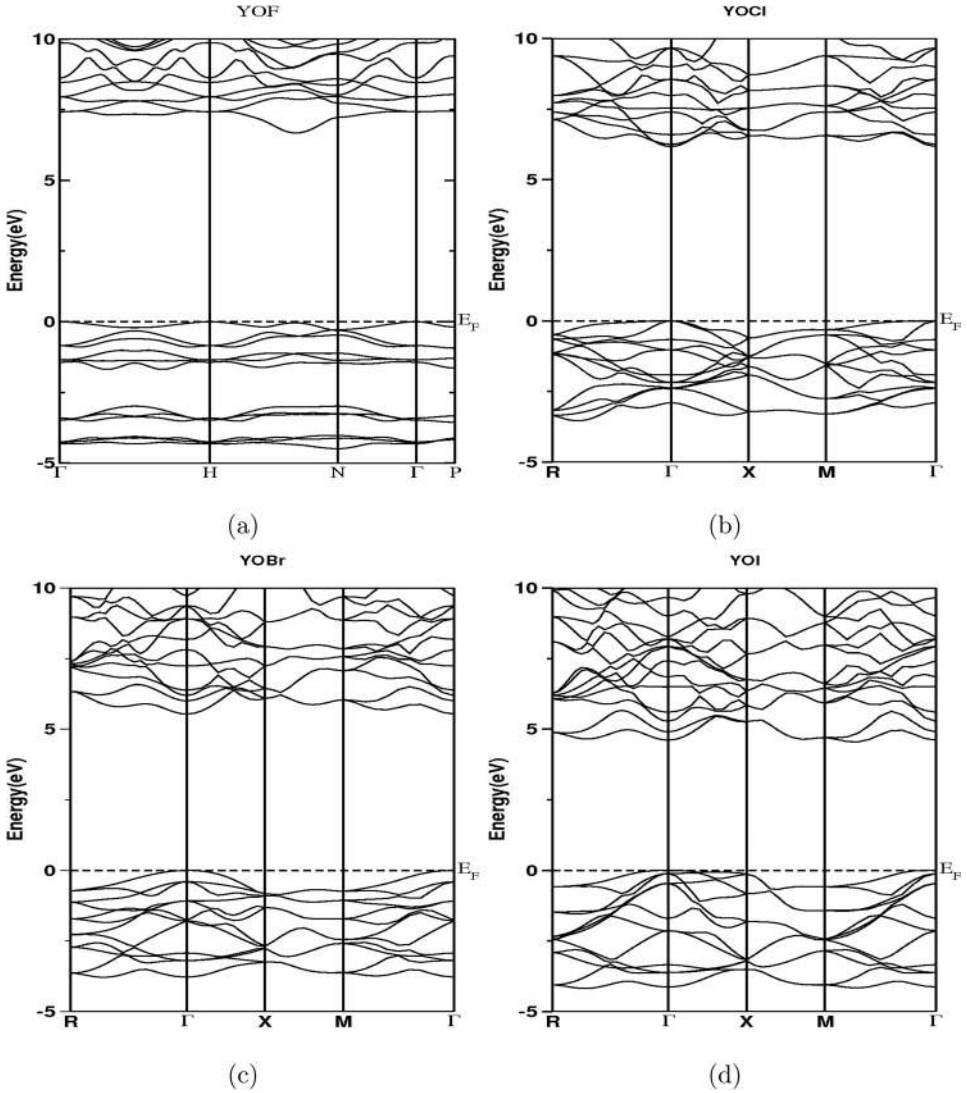

FIG. 2. Calculated band structure of YOX (X = F, Cl, Br, and I) along the high symmetry directions using TB-mBJ functional with WIEN2k code. YOF and YOI are indirect band gap insulators and YOCl and YOI are direct band gap insulators. The band gap values are decreasing from YOF to YOI.

remaining compounds. The energy difference between the second and third blocks decreases from YOCl to YOI. The width of the valence band increases from YOF to YOI. Ryzhkov *et al.*[33,34] found the band gap of YOF to be 5.7 eV, while Lobach *et al.*[35] reported the gap to be 7.2 eV. Our calculated band gap of 6.8 eV is close to these reported values.

B. Mechanical stability

Mechanical stability of the presently studied compounds is analyzed by calculating their elastic constants. Elastic constants are calculated by using the CASTEP code for the optimized crystal structure. These compounds having rhombohedral (YOF) and tetragonal (YOCl, YOBr, and YOI) crystal structures have six independent elastic constants. In the Voight notation, these are C_{11}, C_{12}, C_{13}, C_{14} C_{33}, C_{44} for YOF in the rhombohedral crystal structure, and C_{11}, C_{12}, C_{13}, C_{33}, C_{44}, C_{66} for YOX (X = Cl, Br, and I) compounds in the tetragonal crystal structure. The Born-Huang mechanical stability criterion[36] is given by $C_{11} - |C_{12}| > 0$, $(C_{11} + C_{12})C_{33} - 2C_{13}^2 > 0$, $(C_{11} - C_{12})C_{44} - 2C_{14}^2 > 0$, for rhombohedral structure and $C_{11} > 0$, $C_{33} > 0$, $C_{44} > 0$, $C_{66} > 0$, $(C_{11} - C_{12}) > 0$, $(C_{11} + C_{33} - 2C_{13}) > 0$ and $[2(C_{11} + C_{12}) + C_{33} + 4C_{13}] > 0$ for the tetragonal crystal structure. Clearly, the calculated elastic constants satisfy the Born-Huang criterion indicating that these compounds are indeed mechanically stable. The calculated elastic constants are given in Table II.

C. Vibrational properties

We have calculated the Raman and IR frequencies of all the four YOX compounds. Since all these compounds have two formula units per unit cell, there are three acoustic modes and 15 optic modes. Group-theoretic classification of the optic modes is as follows:

$$YOF : \Gamma = 3A_{1g} + 3E_g + 2A_{2u} + 2E_u$$
$$YOX : \Gamma = 2A_{1g} + 3E_g + B_{2g} + 2A_{2u} + 2E_u,$$

where X = Cl, Br, and I. While the A and B modes are non-degenerate, the E modes are doubly degenerate. Of these, six are Raman active ($3A_{1g} + 3E_g$ for YOF, and $2A_{1g} + 3E_g + B_{2g}$ for YOCl, YOBr, and YOI) and remaining are IR active. These are shown together with the experimental Raman frequencies in Tables III and IV. There is a good agreement between the experiment and calculated Raman frequencies in the low wavenumber region. As can be clearly seen from Fig. 4, replacement of Cl by Br and I results in a

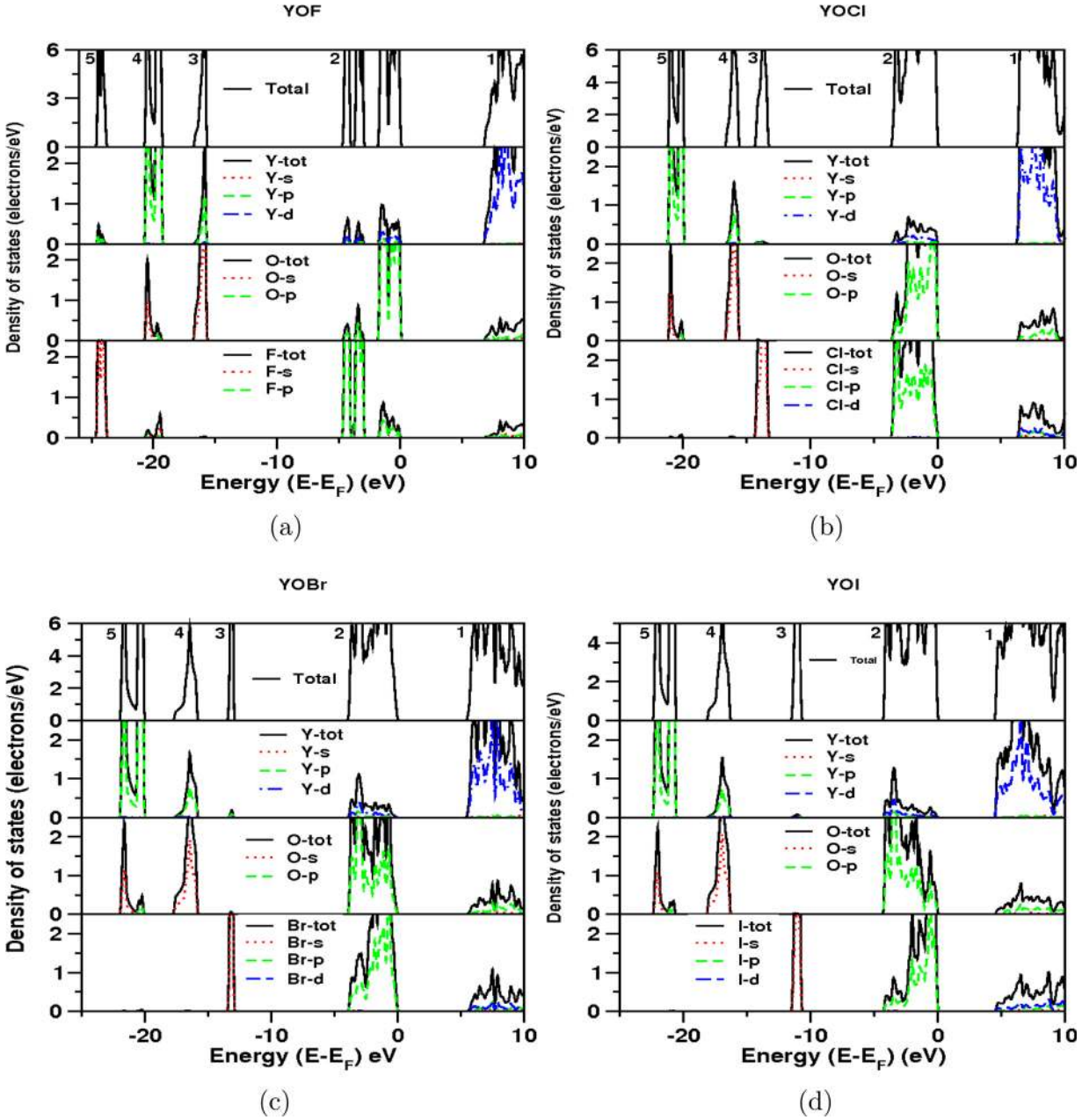

FIG. 3. Partial density of states of YOX (X = F, Cl, Br, and I) compounds calculated using TB-mBJ functional with WIEN2k code. The valence bands are mainly due to hybridized O-*p* and F-*p* states whereas the conduction band is due to Y-*d* states in all the compounds.

red shift of the phonon peak, particularly in the low energy region. The frequencies become smaller on moving from YOF to YOI which is due to increase in the mass of the halides.

All the computed mode frequencies were real. Absence of modes with imaginary frequency clearly shows that all the compounds studied here are dynamically stable. $E_g^{(1)}$, $E_g^{(2)}$, and $E_g^{(3)}$ modes correspond to motion of Y, X (X = F, Cl), and O atoms, respectively, in case of YOF, YOCl whereas in case of YOBr, YOI these modes correspond to displacement of the X (X = Br, I), Y, and O atoms. Similarly the vibrational modes $A_{1g}^{(1)}$, $A_{1g}^{(2)}$ and $A_{1g}^{(3)}$ belong to the antisymmetric vibration of Y, F, and O atoms, respectively, in case of YOF, whereas in case of YOX (Cl, Br, I) $A_{1g}^{(1)}$ and $A_{1g}^{(2)}$ modes correspond to antisymmetric vibration of Y and X (Cl, Br, and I). The B_{2g} mode corresponds to antisymmetric vibration of O atoms.

TABLE II. Elastic constants (C_{ij}, in GPa) of YOX (X = F, Cl, Br, and I) calculated at the theoretical equilibrium volume within LDA.

Compound	C_{11}	C_{12}	C_{13}	C_{14}	C_{33}	C_{44}	C_{66}
YOF	258.5	108.8	105.7	23.8	240.5	94.6	…
YOCl	178.4	59.1	70.3	…	114.4	37.0	72.8
YOBr	157.5	40.4	21.5	…	21.6	20.9	57.7
YOI	143.7	29.6	16.6	…	20.2	8.5	48.4

D. Optical properties

The knowledge of both the real and the imaginary parts, respectively ,ε_1 and ε_2, of the dielectric function allows for

TABLE III. Calculated Raman frequencies in cm^{-1} with LDA and GGA functionals using CASTEP code.

	Mode	YOF	Mode	YOCl (exp[37,38])	Mode	YOBr	Mode	YOI
GGA	$E_g^{(1)}$	142.0	$E_g^{(1)}$	150.9(160, 159)	$E_g^{(1)}$	41.16	$E_g^{(1)}$	36.5
	$A_{1g}^{(1)}$	282.3	$E_g^{(2)}$	202.5(215, 208)	$A_{1g}^{(1)}$	113.7	$A_{1g}^{(1)}$	88.6
	$E_g^{(2)}$	345.2	$A_{1g}^{(1)}$	228.3	$E_g^{(2)}$	153.6	$E_g^{(2)}$	158.7
	$A_{1g}^{(2)}$	400.9	$A_{1g}^{(2)}$	254.8 (260, 259)	$A_{1g}^{(2)}$	272.0	$A_{1g}^{(2)}$	253.6
	$A_{1g}^{(3)}$	522.3	B_{2g}	440.6(375, 373)	B_{2g}	456.2	B_{2g}	437.9
	$E_g^{(3)}$	549.0	$E_g^{(3)}$	606.2(526, 522)	$E_g^{(3)}$	647.4	$E_g^{(3)}$	617.8
LDA	$E_g^{(1)}$	140.9	$E_g^{(1)}$	156.2(160, 159)	$E_g^{(1)}$	128.5	$E_g^{(1)}$	54.3
	$A_{1g}^{(1)}$	294.1	$E_g^{(2)}$	204.4(215, 208)	$A_{1g}^{(1)}$	145.2	$A_{1g}^{(1)}$	96.9
	$E_g^{(2)}$	355.4	$A_{1g}^{(1)}$	242.6	$E_g^{(2)}$	161.2	$E_g^{(2)}$	162.6
	$A_{1g}^{(2)}$	409.5	$A_{1g}^{(2)}$	263.5(260, 259)	$A_{1g}^{(2)}$	252.4	$A_{1g}^{(2)}$	257.4
	$A_{1g}^{(3)}$	522.5	B_{2g}	438.5(375, 373)	B_{2g}	435.9	B_{2g}	430.3
	$E_g^{(3)}$	562.7	$E_g^{(3)}$	613.3(526, 522)	$E_g^{(3)}$	609.9	$E_g^{(3)}$	617.7

the calculation of all the important optical functions such as refractive index, reflectivity, and absorption coefficients. The dielectric function can be calculated, including the excitonic effects, using TDDFT.[30,39,40] We have used the recently developed bootstrap kernel[30,31] within TD-DFT for this purpose. In order to highlight the effect of excitons, we have also calculated the optical spectra without electron-hole effects by using the random phase approximation.

The dielectric functions calculated within RPA using electronic states obtained from TB-mBJ band structure are shown in Fig. 5. ε_2 shows a peak for all materials at ~10 eV and another peak at a higher energy ~30 eV. In all the compounds, the peak in ε_2 at lower energy is due to transition from O-*p* and X-*p* states to the conduction band. ε_1 is also shown in Fig. 5. It is interesting to note that the maximum of the real part of the dielectric function shifts towards lower energies as the atomic number of X increases. This is indicative of the fact that the binding strength decreases on moving from YOF to YOI.

From the real and imaginary parts of the dielectric function, refractive index can be easily determined and it is shown in Fig. 6. Following the trend in $\varepsilon_1(\omega = 0)$, the refractive index of these compounds shows an increase on moving from YOF to YOI. The static refractive index ($n(0)$) along *x* directions of YOF, YOCl, YOBr, and YOI are 1.68, 1.93, 1.94, and 2.0, respectively. We also observe that the anisotropy increases from YOF to YOI which indicates that YOF and YOCl may be much better as ceramic scintillators as compared to YOBr and YOI.

TABLE IV. Calculated IR frequencies in cm^{-1} with LDA and GGA functionals using CASTEP code.

	Mode	YOF	Mode	YOCl	Mode	YOBr	Mode	YOI
GGA	E_u	271.5	E_u	61.7	E_u	58.4	E_u	62.5
	A_{2u}	334.8	A_{2u}	187.9	A_{2u}	146.2	A_{2u}	133.6
	E_u	508.5	E_u	482.9	E_u	513.7	E_u	494.6
	A_{2u}	522.2	A_{2u}	552.1	A_{2u}	622.3	A_{2u}	586.7
LDA	E_u	290.2	E_u	82.9	E_u	82.3	E_u	68.1
	A_{2u}	358.7	A_{2u}	211.1	A_{2u}	127.7	A_{2u}	128.8
	A_{2u}	522.9	E_u	497.9	E_u	493.6	E_u	503.2
	E_u	525.5	A_{2u}	554.0	A_{2u}	548.9	A_{2u}	565.1

The X-ray photoelectron and X-ray emission spectra of YOF were studied by Ryzhkov *et al.*[33,34] and they reported that the main contribution to the maximum intensity peak is the excitation of electrons in Y-4*p* states to the vacant Y-4*d* states. The spectral feature seen in the left and right sides of the maximum intensity peak arises, respectively, due to transition of electrons from F-2*s* and O-2*s* to Y-4*d*. These can be clearly seen in our calculated YOF absorption spectra (Fig. 7) where the highest intensity peak is due to transition from Y-*p* states to the conduction band and the peaks around 35 to 40 eV and 25 eV are due to transition from F-*s* and O-*s* states to the conduction band, respectively. Since the valence band is mainly due to O-*p* states and conduction band is mainly due to Y-*d* states, it is expected that the luminescence has main contribution arising due to the transitions from Y-*d* to O-*p* states supporting the above reports.

The frequency dependent dielectric function of YOX (X = F, Cl, Br, and I) compounds calculated using the TDDFT and the corresponding figures are shown in Fig. 8.

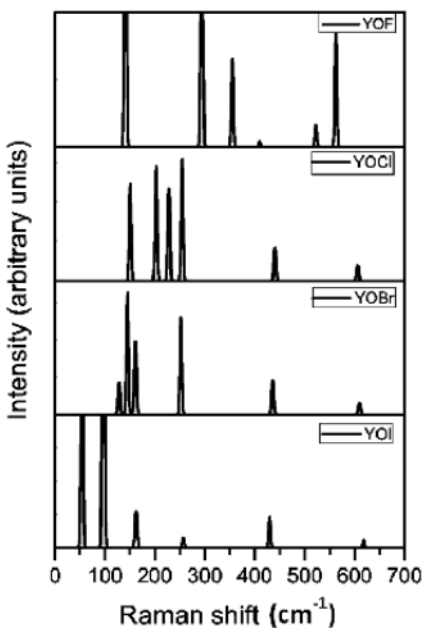

FIG. 4. Raman spectra of YOX compounds using CASTEP code with LDA functional.

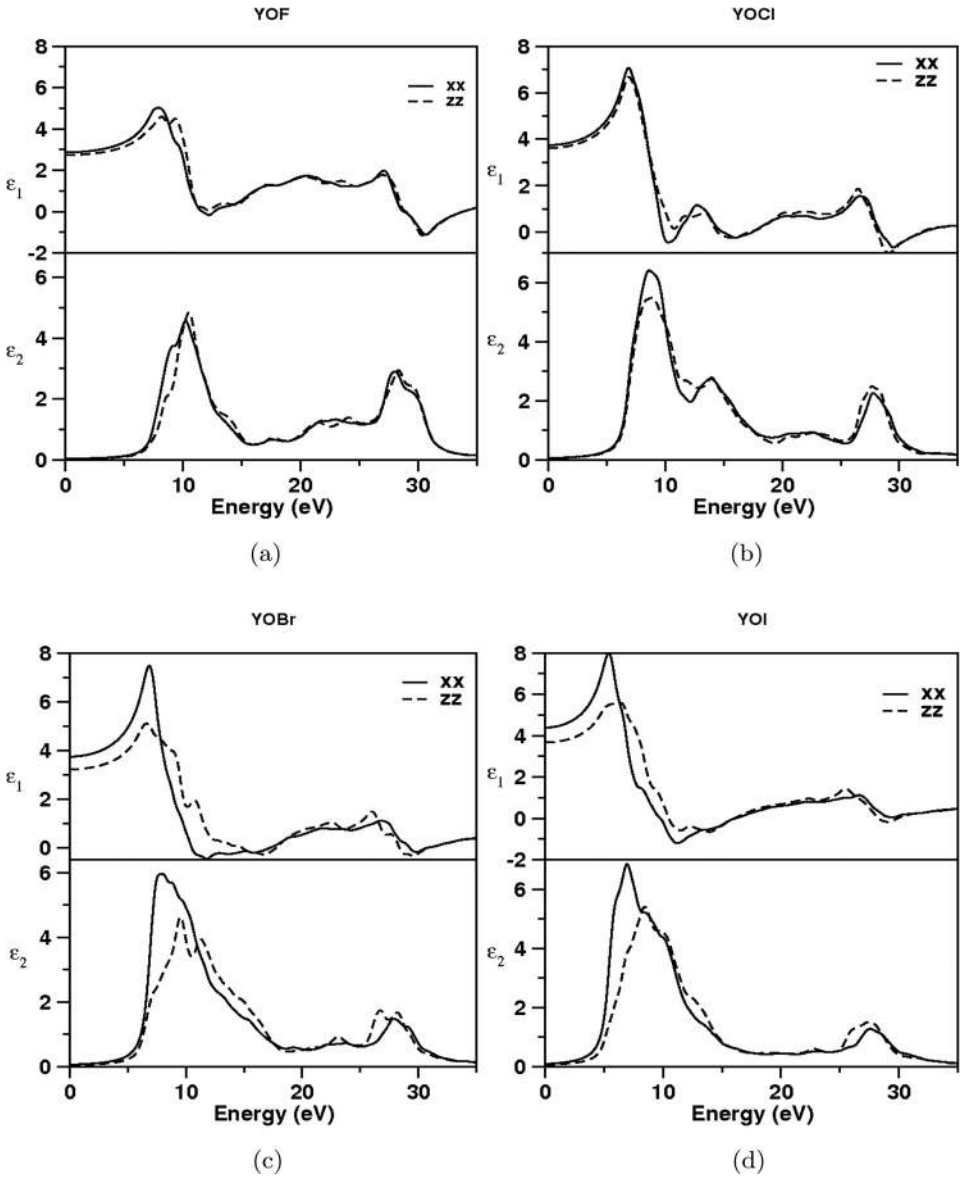

FIG. 5. Calculated dielectric function using TB-mBJ functional with WIEN2k code. The spectra shift to lower energy range on moving from YOF to YOI. xx and zz correspond to ε_{xx}, ε_{zz}.

The TDDFT results for the imaginary part of dielectric function are compared with those of the RPA. We find pronounced excitonic effects in all these materials. The spectral weight at the onset of the absorption is shifted to lower frequencies due to the presence of excitons. This is particulary enhanced in the case of YOF where a strong build up of spectral weight occurs at $\sim$5 eV. $\varepsilon_2(\omega)$ calculated using TDDFT with bootstrap kernel differs significantly from the results obtained using RPA. The ratio of magnitudes of first peak in $\varepsilon_2^{TDDFT}(\omega)$ and $\varepsilon_2^{RPA}(\omega)$ is 6 for YOF and 2 for YOI. These differences are attributed to excitonic effects.

The knowledge of the type of exciton (Wannier vs. Frenkel), and its binding energy is of interest in getting insight into what is happening in the system. Signature of bound excitons is occurrence of discrete absorption peaks below the quasiparticle gap in the optical spectrum. In the case of the oxyhalides studied here, the first peak in the computed $\varepsilon_2^{TDDFT}(\omega)$ is very close to the quasiparticle gap. Since the width of the absorption peak is not too small compared to the distance of the peak from the gap edge, it is not possible to accurately determine the binding energy of the excitons from the computed spectra of the oxyhalides studied here.

An alternative would be to directly calculate exciton binding energy following the Casida equation type TDDFT calculation described by Yang and Uhlrich.[41] They have shown that while the results obtained using the bootstrap kernel is generally accurate for Frenkel excitons, it is not good enough for Wannier excitons.

On the other hand, we know that the Wannier equation

$$\left(-\frac{\hbar^2}{2m_*}\nabla_i^2 - \frac{1}{\epsilon r}\right)\psi(r) = E\psi(r) \tag{1}$$

despite its apparent crudeness, provides reasonably accurate values of binding energy of excitons in many common semiconductors provided the effective Bohr radii of the excitons are much greater than the lattice constant. This is because of the fact that Eq. (1) follows from the Bethe Salpeter equation in the limit of large exciton radius. We took the view that if the exciton radius estimated using the effective mass and static dielectric constant happens to be large, then the

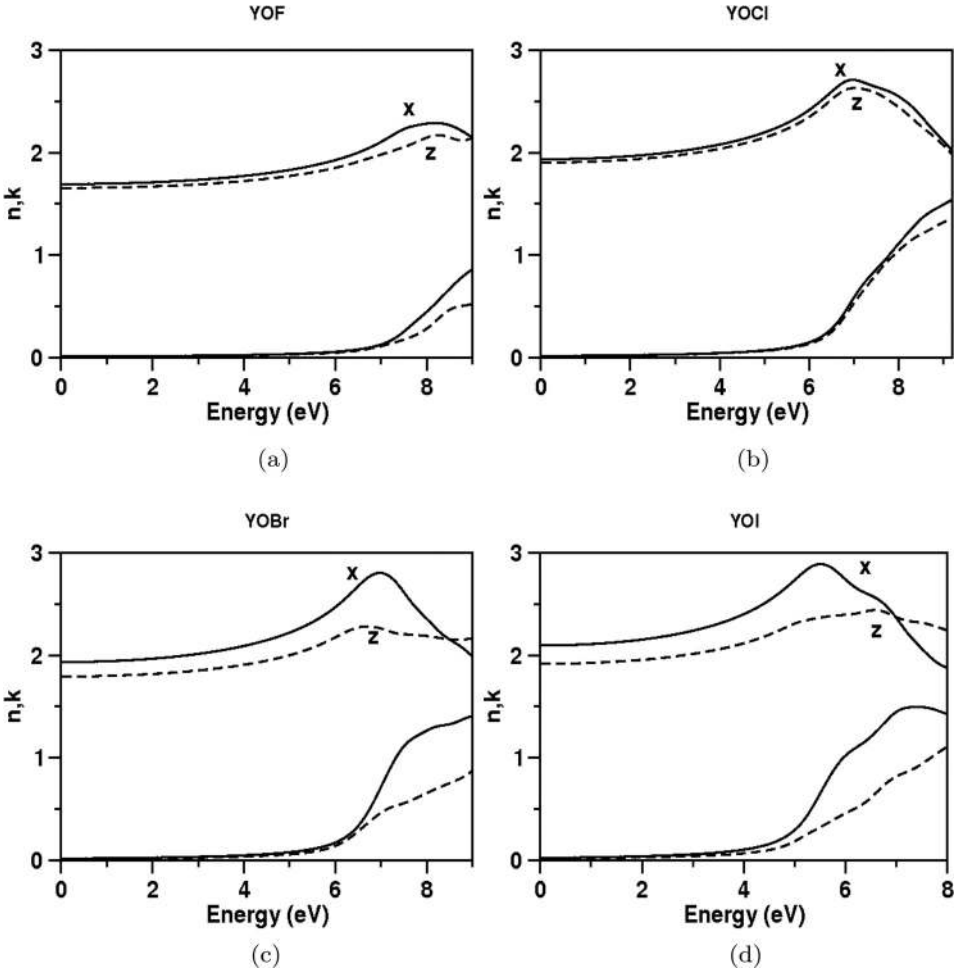

FIG. 6. Refractive index of YOX compounds along the three directions. The value of static refractive index increases from YOF to YOI. x and z correspond to n_{xx}, n_{zz}.

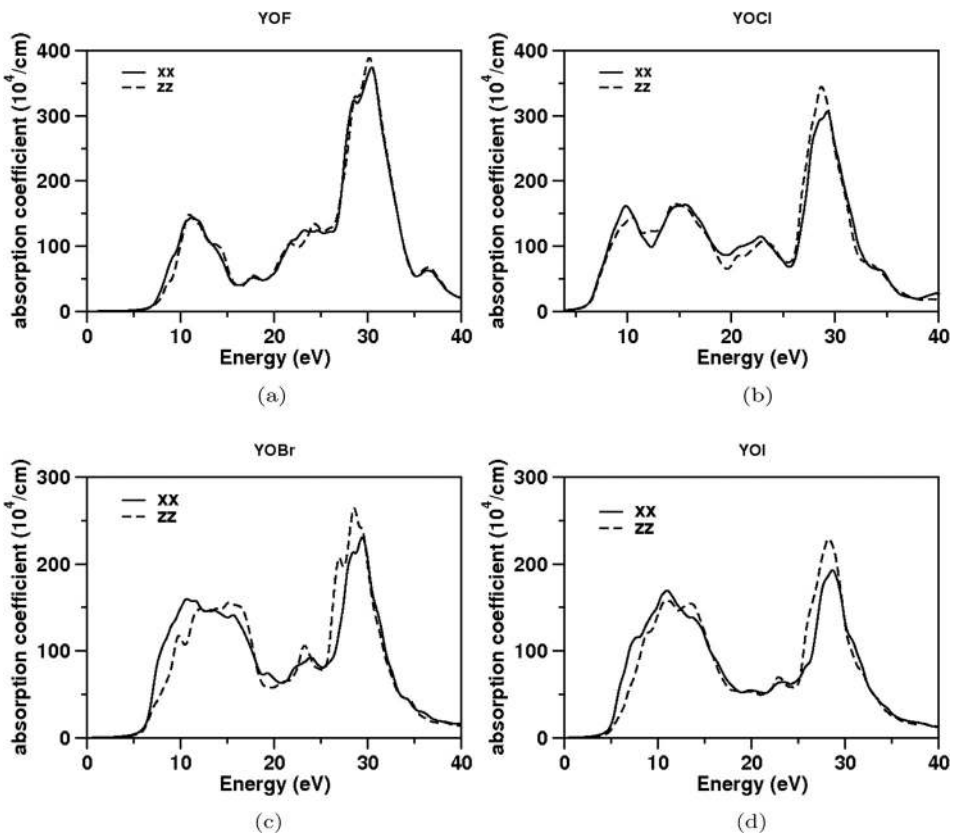

FIG. 7. Absorption spectra calculated using TB-mBJ. xx and zz correspond to α_{xx}, α_{zz}.

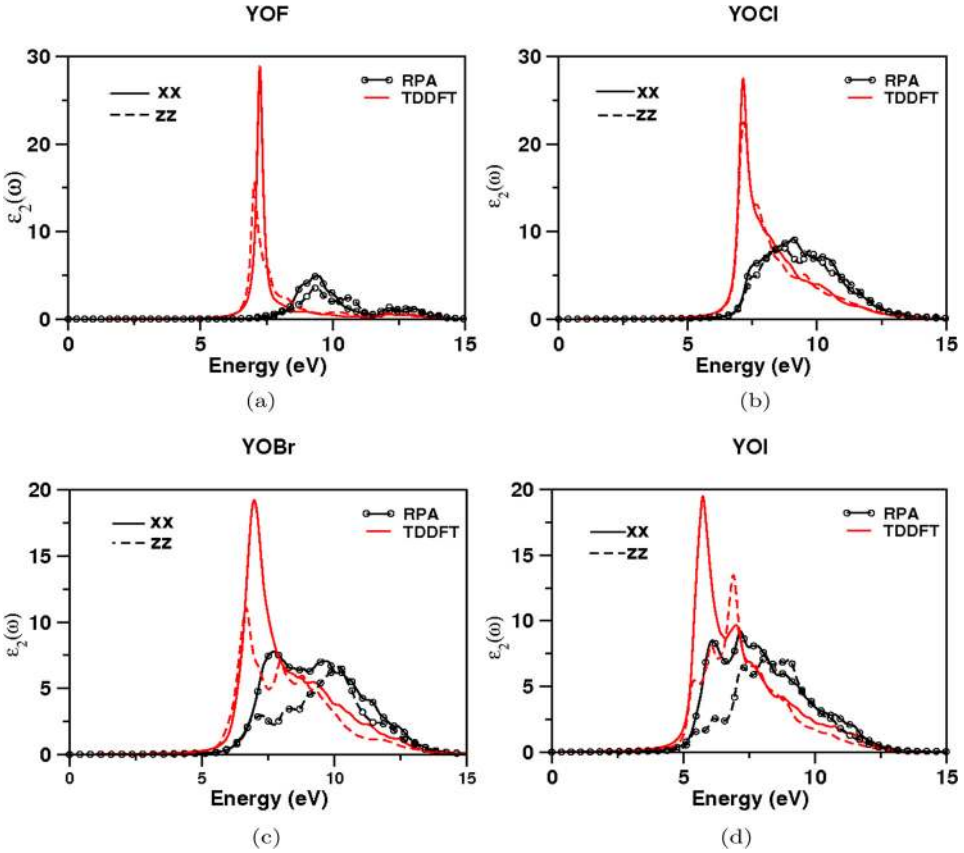

FIG. 8. Imaginary part of dielectric function $\varepsilon_{2,xx}$, and $\varepsilon_{2,zz}$ using elk code, shift of TDDFT spectra from RPA is more for YOF than other compounds.

excitons are of the Wannier type. It also follows that the binding energy calculated by this approach should then be a reasonable first estimate. The results of the calculations indeed show that we have Wannier type excitons in the oxyhalides studied here.

We found the effective reduced mass for the electron-hole pair to be 2.38, 0.51, 0.73, 0.67 (in units of the bare electron mass m_e), respectively, for YOF, YOCl, YOBr, and YOI based on TB-mBJ calculations. The dielectric function has two parts: the electronic and ionic parts. Based on the CASTEP calculations within RPA, it is found that the ionic part $\epsilon_I(0)$ of the static dielectric function $\epsilon(0)$ is much larger than the electronic part $\epsilon_e(0)$ for all the compounds studied here. Specifically, $\epsilon_I(0) = 5.84$, 15.37, 10.72, and 9.0 whereas $\epsilon_e(0) = 2.85$, 3.73, 3.7, 4.3, respectively, for YOF, YOCl, YOBr, and YOI. We have calculated the electronic part of the dielectric function using TDDFT. $\epsilon_e(0)$ calculated using TDDFT are 2.33, 4.24, 4.27, and 4.93, respectively, for YOF, YOCl, YOBr, and YOI. Thus, the difference between the electronic part of the static dielectric function obtained from RPA and TDDFT is found to be small. A similar trend can be expected for the ionic part of the static dielectric function. In view of this, we take the total static dielectric constant given by CASTEP within RPA for estimation of the binding energy of the excitons. Based on these values, we obtained the exciton binding energy to be 0.43, 0.02, 0.04, and 0.05 eV, respectively, for YOF, YOCl, YOBr, and YOI. Excitonic binding energy is more for YOF than the remaining compounds.

Canning *et al.*[4,6,42,43] developed three theoretical criteria for scintillation and luminescence to predict the brightness of Ce^{3+} activated scintillation. These involve (1) the size of the band gap, (2) the energy difference between the valence band maximum (VBM) of the host and the Ce 4*f* level, and (3) the level of localization of the states with *d*-character of the excited state. The first criterion is related to the number of electron-hole pair produced with an incident gamma ray which is inversely proportional to the band gap. So, the band gap of host compound should be as small as possible and also should accommodate the Ce 4*f* and 5*d* states. Criterion 2 is related to energy difference between 4*f* and VBM-if it is large there will be low probability of transferring holes from host to Ce sites via thermal excitation which in turn will reduce the brightness. Criterion 3 is all about the *d* character of the excited state which could be due to the host or the Ce-*d* states. If it has Ce-*d* character, we can observe bright scintillation from Ce 4*f* to 5*d* states. In our case, we found the band gap to decrease from YOF to YOI. Therefore, we can expect the electron hole pair production to increase from YOF to YOI, and energy difference between Ce 4*f*-VBM to decrease from YOF to YOI. So, we can expect luminosity to increase from YOF to YOI which supports the earlier reports.[5,6] Moreover, the width of the lower energy absorption band (or imaginary part of the dielectric function) increases from YOF to YOI because of which the number of electrons available for excitation also increases and leads to increased luminescence which also supports the earlier reports. This may be one of the reasons for the increase in the luminescence from YOF to YOI. This is because formation of exciton increases the possibility of electron-hole pairs getting trapped near impurities which leads to increase in the non radiative transition thereby decreasing the luminescence.

Chaudhry *et al.*[6] calculated the Ce-doped level in Y and La oxyhalides, and also found that YOF:Ce compound has good localization of the excited states but the large band gap of YOF eventually reduces the number of electron hole pairs whereas in YOBr:Ce, and YOI:Ce compounds better localization of the excited states, lower band gap, small 4*f*-VBM separation (compared to YOCl which resembles YOF) would lead to bright Ce-activated scintillation in YOBr and YOI. As the luminosity increases from Cl to I, YOBr and YOI can act as good host compounds among the studied oxy-halides.

IV. CONCLUSIONS

We have studied the electronic, optical, and vibrational properties of YOX (X = F, Cl, Br, and I) compounds. We found the van-der-Waals effect to be almost negligible in these compounds except for YOBr. YOX compounds have a comparable light-output to Cerium doped rare-earth halides, while they are much more stable than halides with respect to hygroscopic character. Because of their high densities these materials are also better for absorbing radiation. YOX compounds are good candidates for host materials (for rare earth doping) and show increased luminescence on moving from F to I. The calculated dielectric function and refractive index showed decrease in isotropy from YOF to YOI. We have also calculated the optical properties using the newly developed bootstrap kernel which includes the excitonic effects and we find that these materials show strong excitonic features in the absorption spectra especially in the case of YOF.

ACKNOWLEDGMENTS

V.K. acknowledges IIT Hyderabad for the HPC facility. G.S. acknowledges IIT Hyderabad, and NPSF CDAC (PUNE) for the computational facility and MHRD for fellowship. G.S. and V.K. acknowledge S. Sharma (Max-Planck-Institut für Mikrostrukturphysik, Weinberg 2, D-06120 Halle, Germany) for the useful discussions.

[1]E. V. D. Van Loef, P. Dorenbos, C. W. E. Van Eijk, K. Kramer, and H. U. Gudel, Nucl. Instrum. Methods Phys. Res. A **486**, 254 (2002).
[2]P. R. Menge, G. Gautier, A. Iltis, C. Rozsa, and V. Solovyev, Nucl. Instrum. Methods Phys. Res. A. **579**, 6 (2007).
[3]P. Dorenbos, Phys. Status. Solidi A **202**, 195 (2005).
[4]R. Boutchko, A. Canning, A. Chaudhry, R. Borade, E. Bourret-Courchesne, and S. E. Derenzo, IEEE Trans. Nucl. Sci. **56**, 977 (2009).
[5]Y. D. Eagleman, E. Bourret-Courchesne, and S. E. Derenzo, J. Lumin. **131**, 669 (2011).
[6]A. Chaudhry, A. Canning, R. Boutchko, Y. D. Porter-Chapman, E. Bourret-Courchesne, S. E. Derenzo, and N. G. Jensen, IEEE Trans. Nucl. Sci. **56**, 949 (2009).
[7]A. W. Mann and D. J. M. Bevan, Acta Crystallogr. B **26**, 2129 (1970).
[8]I. Levin, Q. Z. Huang, L. P. Cook, and W. Wong-Ng, Eur. J. Inorg. Chem. **2005**, 87 (2005).
[9]G. Meyer and T. Staffel, Z. Anorg. Allg. Chem. **532**, 31 (1986).
[10]Institute of Experimental Mineralogy Russian Academy of Sciences, 142432, Chernogolovka, Moscow district, A. V. Chichagov, http://database.iem.ac.ru/mincryst/inf.php?bismocl.it3.
[11]M. D. Segall, P. J. D. Lindan, M. J. Probert, C. J. Pickard, P. J. Hasnip, S. J. Clark, and M. C. Payne, J. Phys.: Condens. Matter. **14**, 2717 (2002).
[12]S. J. Clark, M. D. Segall, C. J. pickard, P. J. Hasnip, M. J. Probert, K. Refson, and M. C. Payne, Z. Kristallogr. **220**, 567 (2005).
[13]M. C. Payne, M. P. Teter, D. C. Allan, T. A. Arias, and J. D. Joannopoulos, Rev. Mod. Phys. **64**, 1045 (1992).
[14]P. Blaha, K. Schwarz, P. I. Sorantin, and S. B. Tricky, Comput. Phys. Commun. **59**, 399 (1990).
[15]P. Blaha, K. Schwarz, G. K. H. Madsen, D. Kvasnicka, and J. Luitz, *WIEN2K, An Augmented Plane Wave Plus Local Orbitals Programe for Calculating Crystal Properties* (Karlheinz Schwarz, Techn. Universität Wien, Austria), 2001.
[16]See http://elk.sourceforge.net, 2004.
[17]D. M. Ceperley and B. J. Alder, Phys. Rev. Lett. **45**, 566 (1980).
[18]J. P. Perdew and A. Zunger, Phys. Rev. B **23**, 5048 (1981).
[19]J. P. Perdew, K. Burke, and M. Ernzerhof, Phys. Rev. Lett. **77**, 3865 (1996).
[20]F. Ortmann, F. Bechstedt, and W. G. Schmidt, Phys. Rev. B **73**, 205101 (2006).
[21]A. Tkatchenko and M. Scheffler, Phys. Rev. Lett. **102**, 073005 (2009).
[22]S. Grimme, J. Comput. Chem. **27**, 1787 (2006).
[23]S. Grimme, J. Comput. Chem. **25**, 1463 (2004).
[24]T. Bucko, J. Hafner, S. Lebegue, and J. G. Angyan, J. Phys. Chem. A **114**, 11814 (2010).
[25]K. Rapcewicz and N. W. Ashcroft, Phys. Rev. B **44**, 4032 (1991).
[26]H. Ding, K. G. Ray, V. Ozolins, and M. Asta, Phys. Rev. B **85**, 012104 (2012).
[27]D. J. Singh, Phys. Rev. B **82**, 205102 (2010).
[28]D. Koller, F. Tran, and P. Blaha, Phys. Rev. B **83**, 195134 (2011).
[29]M. J. Mehl, J. E. Osburn, D. A. Papaconstantopoulus, and B. M. Klein, Phys. Rev. B **41**, 10311 (1990).
[30]S. Sharma, J. K. Dewhurst, A. Sanna, and E. K. U. Gross, Phys. Rev. Lett. **107**, 186401 (2011).
[31]S. Sharma, J. K. Dewhurst, A. Sanna, A. Rubio, and E. K. U. Gross, New J. of Phys. **14**, 053052 (2012).
[32]H. Xiao, J. T. Kheli, and W. A. Goddard, J. Phys. Chem. Lett. **2**, 212 (2011).
[33]M. V. Ryzhkov, V. A. Gubanov, D. E. Ellis, A. L. Hagstrum, and E. Z. Kurmaev, Physica B+C **101**, 364 (1980).
[34]M. Rizhkov, V. A. Gubanov, M. P. Bytzman, A. L. Hagstrom, and E. Z. Kurmaev, J. Electron Spectrosc. Relat. Phenom. **18**, 227 (1980).
[35]V. A. Lobach, B. V. Shulgin, I. N. Shabanova, V. A. Trapezmkov, N. P. Sergushm, and A. A. Sobol, Sov. Solid. State. Phys. **20**, 2002 (1978).
[36]M. Born and K. Huang, *Dynamical Theory of Crystal Lattice*, (Oxford University Press, Oxford, 1998).
[37]R. Withnall, J. Silver, P. J. Marsh, and G. R. Fern, *Wolfson Centre for Material Processing* (Brunel University, Kingston Lane, Uxbridge, Middlesex, UK).
[38]J. Holsa, E. Kestila, K. Koski, and H. Rahiala, J. Alloys Compd. **225**, 193 (1995).
[39]L. Reining, V. Olevano, A. Rubio, and G. Onida, Phys. Rev. Lett. **88**, 066404 (2002).
[40]S. Botti, F. Sottile, N. Vast, V. Olevano, L. Reining, H.-C. Weissker, A. Rubio, G. Onida, R. D. Sole, and R. W. Godby, Phys. Rev. B **69**, 155112 (2004).
[41]Z.-h. Yang and C. A. Ullrich, Phys. Rev. B **87**, 195204 (2013).
[42]A. Canning, R. Boutchko, A. Chaudhry, and S. E. Derenzo, IEEE Trans. Nucl. Sci. **56**, 944 (2009).
[43]A. Canning, A. Chaudhry, R. Boutchko, and N. Grønbech-Jensen, Phys. Rev. B **83**, 125115 (2011).